Dynamic Characteristic Evaluation of the Hybrid Electric Vehicle by Simulation

Suryanto
Department of Mechanical, The State Polytechnic of Ujung Pandang, Jln. Perintis Kemerdekaan, Makassar, Indonesia

Keywords: Drivability, Simulation, Hybrid Electrical Vehicle, Dynamic, Response.

Abstract: The development and implementation of hybrid electric vehicles (HEVs) have taken an accelerated pace. However, one of the critical issues for this vehicle typology is drivability, which relates to driving comfort. The objective of this study is to evaluate the dynamic characteristic of the four wheels drive parallel hybrid electrical vehicle under transient conditions, particularly during tip-in and tip-out maneuvers. The evaluation of the vehicle dynamic was carried out by using MATLAB/Simulink simulation to predict a wide range of vehicle dynamic behavior. The model has been developed to allow the sensitivity analysis of some parameters which affect the layout of the powertrain. The vehicle dynamic response behavior has high oscillations and a more complex time history during hybrid mode due to the combination of rapidly variable torque demand and the first natural frequencies from two different propulsions in transient condition. It was found that in many cases the engine drivetrain makes a greater contribution to the oscillation than the electric motor drivetrain.

1 INTRODUCTION

A hybrid electric vehicle propulsion system typically consists of an internal combustion engine (ICE), a fuel tank, one or more electric motor (EM), electrical energy storage systems (e.g. batteries, super-capacitors), power converters, transmissions and driveline linkages.

The combination of an EM and ICE in a hybrid vehicle could be configured in several ways. There are three well known types of HEV configurations. These are: (a) series, (b) parallel and (c) series-parallel configurations. In the case of a vehicle with parallel four wheels drive hybrid electric vehicle (4WD HEV) powertrain architecture; there are some variations that might be implemented (Giancarlo and Lorenzo 2019). The selection will depend on the type of vehicle application, e.g. SUV, truck, passenger car or bus. A 4WD HEV or the dual drive vehicle as studied here combines an internal combustion engine that drives the front wheels and an electric motor that drives the rear wheels as shown in Figure 1.

(Liao et al. 2004), who has studied modeling and analysis of some concepts (architecture) relating to the application of power train 4WD HEV, determines that the configuration of such a powertrain as shown in Figure 1 is the easiest and full hybrid architecture system. A benefit of this approach is that the conversion of a conventional powertrain into a hybrid powertrain can be accomplished with minimal modification. Another author (Rizzoni and Guzzella 2019), states that, this architecture concept is the simplest form of a parallel HEV.

Based on the powertrain configuration outlined, a 4WD HEV has the following four operational modes: Electric Vehicle, ii) Engine Mode: iii) Braking Regenerative Mode: iv) Four Wheel Drive (4WD) Parallel Hybrid Mode.

The drivability of a vehicle during tip-in/tip-out or gearshift maneuvers is affected by several parameters. In particular, the low frequency drivability of a vehicle is generally measured through acceleration and jerk profiles (Velazquez and Assadian 2019).

Suryanto, .
Dynamic Characteristic Evaluation of the Hybrid Electric Vehicle by Simulation.
DOI: 10.5220/0010967000003260
In *Proceedings of the 4th International Conference on Applied Science and Technology on Engineering Science (iCAST-ES 2021)*, pages 1440-1447
ISBN: 978-989-758-615-6; ISSN: 2975-8246

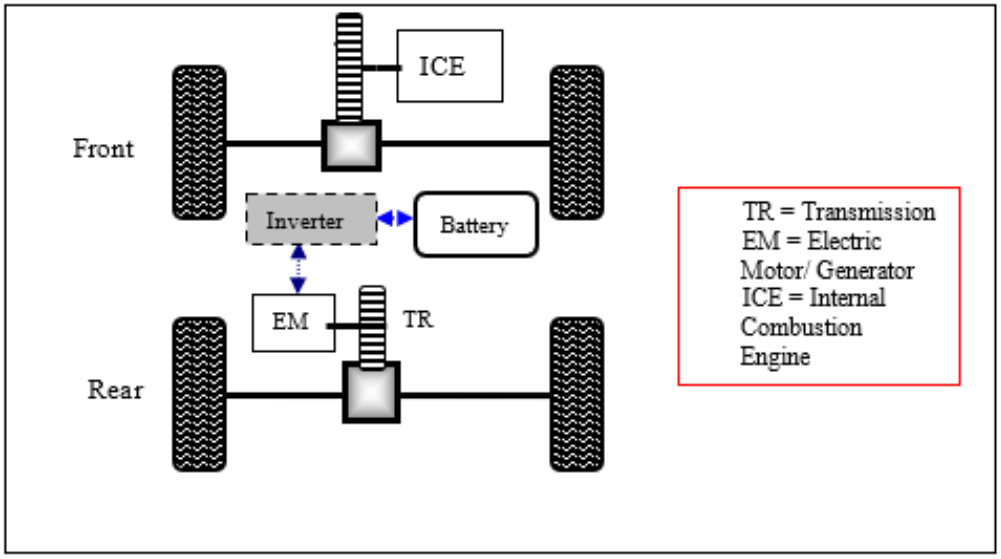

Figure 1: Schematic of the parallel powertrain architecture a 4WD of HEV.

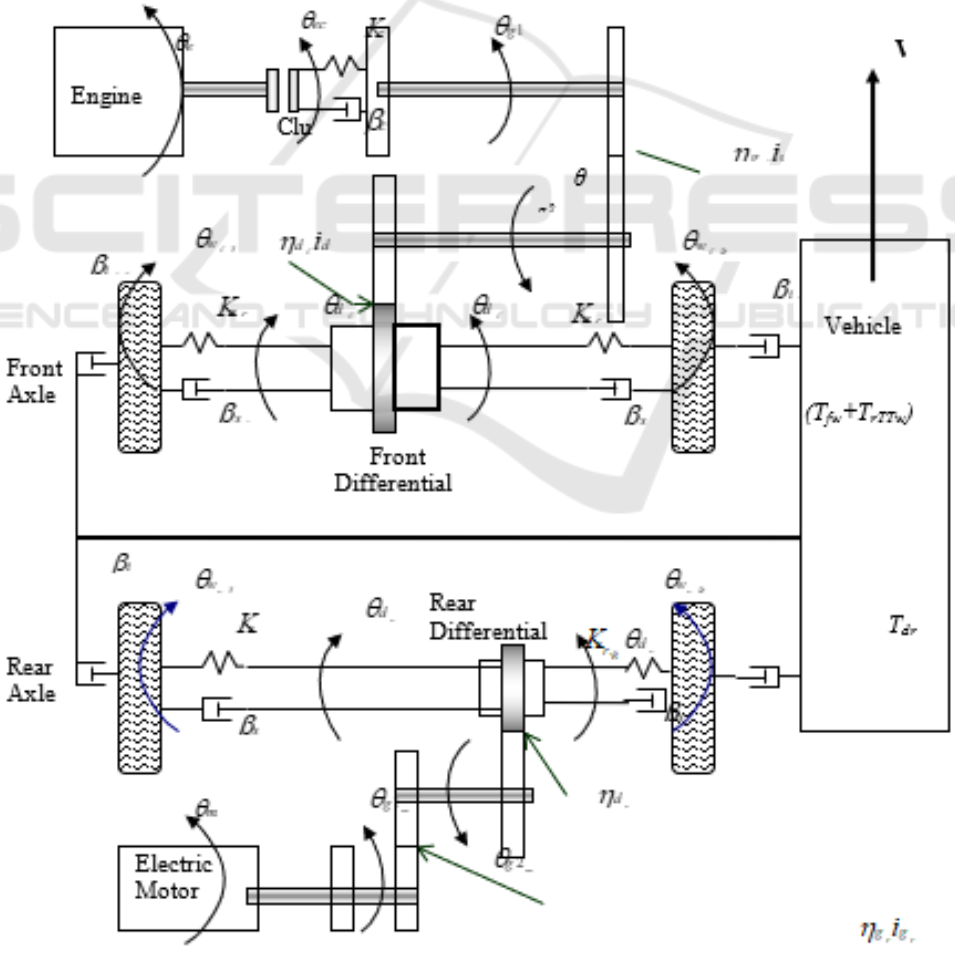

Figure 2: The schematic of the complex model of the 4WD HEV.

- The longitudinal acceleration characteristic is the main parameter which affects drivability (Hohn and Stahl, 2011). Longitudinal acceleration is associated with response delay, overshoot, rise rate, jerk, and kick.
- Jerk (J_k) is the time rate of change in the vehicle longitudinal acceleration $\ddot{X}_{sm}$. In mathematical terms, jerk is defined as the derivative of longitudinal acceleration and is written as:

$$J_k = \frac{\ddot{X}_{m_v}}{d_t} \quad (1)$$

- Kick (K_k) is the first decrease of longitudinal acceleration. It can be expressed as:

$$K_k = A_{1,\max} - A_{1',\min} \quad (2)$$

Where $A_{1,\max}$ and $A_{1',\min}$ are the first peak high and peak low overshoots.

- Rise time (t_r) is the time required for the response to rise from 10% to 90 % (rise rate) of the steady-state value. This is the initial part of vehicle response during gearshift or tip-in.
- Overshoot (O_v) the time required for the response to settle within a certain range of the steady-state is called the settling time.

2 MODELING DEVELOPMENT OF THE FOUR-WHEEL-DRIVE HYBRID ELECTRIC VEHICLE

The model will first be presented with a model structure and detailed description of the mechanical layout including governing equations. Mathematical models that predict the vehicle dynamic performances are created systematically in order to evaluate the dynamic low frequency behavior. In particular, the aim of the modeling is to determine the most important dynamic physical parameters of the vehicle that affect drivability during the investigated transient conditions.

The studied model layout of the 4WD HEV is depicted in Figure 2. The front powertrain in the vehicle consists of an ICE coupled to a six speed automated manual transmission through the friction clutch. The output of the transmission drives the front wheels through a pair of half-shafts. For the rear powertrain, an EM is coupled to the rear axle and drives the rear wheels through a two-speed transmission integrated with the differential.

2.1 Engine Model

The engine is modeled through experimental maps, which generate a theoretical engine torque as a function of throttle position and engine speed. The engine dynamics are determined through a first order transfer function that depends on the engine characteristic (e.g. time constant). The output of the transfer function is the delayed torque (T_{de}), which is used for the moment balance equation of the engine shaft.

For a body with constant moment inertia rotating about a fixed axis, Newton's second law of motion is often referred that can be stated mathematically according to:

$$\sum_i T_{ext_i} - J\ddot{\theta} = 0 \quad (3)$$

Where the summation over i includes all torques acting on the body (T_{ext}); J is the moment of inertia and $\ddot{\theta}$ is the angular acceleration.

Based on Newton's law, the sum of the torques acting on the engine and the clutch is satisfied by the following equation:

$$T_{de} - T_{ec} = J_e\ddot{\theta}_e \quad (4)$$

Where T_{de} is the delayed engine torque and T_{ec} is the engine clutch torque damper, J_e is the engine moment inertia including the fly-wheel moment of inertia, and $\ddot{\theta}_e$ is the angular acceleration of the engine.

Engine Gearbox Model

Primary shaft: The damping of the system transmission of the gear box may be neglected altogether (Cavallino and Turner, 2009).

The primary shaft torque is determined as:

$$T_{g1} = T_{ec} - J_{g1}\ddot{\theta}_{g1} \quad (5)$$

where T_{g1} and J_{g1} are the primary shaft torque at the front transmission and the inertia of the primary shaft respectively; $\ddot{\theta}_{g1}$ is the angular acceleration of the primary shaft of the front transmission.

Secondary shaft: With the front driven axle, the gear on the secondary shaft is connected to the differential directly without using a propeller shaft as shown in Figure 2. The gearbox losses (caused by the internal friction) are represented by the lumped efficiency (η_{g_f})

The secondary shaft torque is determined:

$$T_{g2} = T_{d_{f,i}} + J_{g2}\ddot{\theta}_{g2} \quad (6)$$

Where $T_{d_{f,i}}$ is the input shaft torque of the front differential and T_{g2} is the secondary shaft torque, J_{g2} is the moment inertia of the secondary shaft and $\ddot{\theta}_{g2}$ is the secondary shaft angular acceleration.

Differential and Drive Shaft Model: In the same way as the gearbox transmission, the differential is characterized by a gear ratio. The relation of the differential input and output torque is simply determined by considering the differential conversion ratio and efficiency which is given,

$$T_{d_{f,0}} = T_{d_{f,i}}\eta_{d_f} i_{d_f} \quad (7)$$

Where $T_{d_{f,0}}$ is the output torque of the front differential i_{d_f} is the front gear differential ratio and η_{d_f} is the differential efficiency. The differential loss

The differential output torque is transmitted by two different shafts (right and left shaft), each of which is connected to the wheel through the half-shafts. Since the right half-shaft is asymmetrical with the left half-shaft (the right and the left properties are not the caused by the internal friction) is represented by the lumped efficiency.

The differential output torque is transmitted by two different shafts (right and left shaft), each of which is connected to the wheel through the half-shafts. Since the right half-shaft is asymmetrical with the left half-shaft (the right and the left properties not the same), the torque balances on the differential and half-shafts are expressed as:

$$Td_{f,i}\eta d_f i d_f - Ts_{f,R} - Ts_{f,L} = [Jd_f + 0.5(Js_{f,R} + Js_{f,L})]\ddot{\theta} d_f \quad (8)$$

Where $\ddot{\theta}_{d_f}$ is the differential angular acceleration, $T_{s_{f,R}}$ and $T_{s_{f,L}}$ are the right and left half-shaft torque, J_{d_f}, $J_{s_{f,R}}$, $J_{s_{f,L}}$ are the moment inertia of the differential, the right and left half-shaft, respectively.

1. Front Tyre Model: The wheel model is characterized as a non-linear model. In this case, the longitudinal traction forces (F_x) are modeled by using the Pacejka's Magic Formula (Pacejka, 2006).

The moment balance on the half-shaft to the wheel is required in order to find the wheel angular acceleration which is derived in the following equation.

$$T_{s_{f,R}} - T_{w_{f,R}} - T_{roll_{f,R}} = (J_{w_{f,R}} + J_{s_{f,R}})\ddot{\theta}_{w_{f,R}} \quad (9)$$

Where, $T_{w_{f,R}}$ is the right front wheel torque and $J_{w_{f,R}}$ is the tyre moment inertia.

The wheel torque performance is the function of the longitudinal traction force (F_x) and wheel radius (R_w). Hence, the tyre traction torque can be written as:

$$T_{w_{f,R}} = F_x R_w \quad (10)$$

$T_{roll_{f,R}}$ is the right front tyre rolling resistance torque non-linear model, which is expressed as:

$$T_{roll_{f,R}} = w_v R_w{}^3 (c_{r0} + c_{r1}\dot{\theta}_{w_{f,R}} + c_{r2}\dot{\theta}_{w_{f,R}}{}^2) \quad (11)$$

where c_{r0} is the coefficient of the tyre, c_{r1} is the coefficient of tyre pressure, c_{r2} is the rolling resistance coefficient depending on vehicle velocity square, and w_v is the vertical load for each wheel.

2.2 Electric Motor Axle Drivetrain Model

The electric motor rear axle is modeled as a two-speed gear. Due to the absence of a clutch damper, the rear powertrain is a one degree of freedom system in conditions of constant gear and two degrees of freedom when the internal dynamics of the differential gear set are considered.

2. Electric Motor Model: The EM is modeled in a similar way to the engine model which is found experimentally attained maps that generate a theoretical motor torque as a function of the pedal position and motor speed. The EM dynamics are also determined through a first order transfer function that depends on motor dynamics. The output of the transfer function is the delayed motor torque (T_m).

The Electric Motor Transmission System:
The transmission utilizes a seamless shift system. There are two kinds of clutch to provide a smooth shifting man oeuvre; 1) a one-way sprag clutch for transferring torque to the first gear, and 2) a friction clutch to deliver torque to the second gear. On the sprag clutch, there is a locking ring device, which can prevent the one-way sprag clutch from overrunning when the direction of torque through

the transmission is reversed in order to allow regenerative energy recovery whilst decelerating in first gear (Holdstock et.al 2012). The clutch is electro-hydraulically controlled through the use of a remote brushless motor driven actuator, pressurizing a master cylinder mechanically connected to the Belleville spring of the friction clutch (Alcantar and Assadian 2019). The moment balance equations of the transmission shafts differ for each selected gear due to the effect of the moment of inertia of the two clutches mounted in the different shafts. Therefore, the derivation for first gear and second gear dynamic equations are determined in a different manner. The first gear: when the clutch is engaged, the motor torque will be transferred to the primary shaft. In this condition, the sprag clutch engages while the friction clutch disengages. The torque balance equation for the first gear on the primary shaft which is subjected to the motor torque is:

$$T_m = T_{fc} + (J_m + J_1)\ddot{\theta}_m - T_{g1} \quad (12)$$

where T_m is the motor torque and T_{fc} the motor friction clutch torque, T_{g1} is the primary shaft torque, J_m is the moment of inertia of the motor, J_1 the moment of inertia of the primary shaft, and $\ddot{\theta}_m$ is the angular acceleration of the motor.

The second gear: The moment balance equation forthe primary shaft (in secondary gear selected) is expressed as:

$$T_m = (J_{1b} + J_m + J_1)\ddot{\theta}_m + T_{g2} + T_{g1} \quad (13)$$

Where, T_{g2} is the torque through the second gear and J_{1b} is the moment of inertia of clutch.

3. Gear Box and Differential Model:

The moment balance equations of the transmission shafts differ for each selected gear, therefore the derived differential accelerations in gear one and two are given below.

The first gear: The moment balance equation for the primary shaft is given:

$$T_{g1}i_1\eta_1 + T_{g2}i_2\eta_2 - T_{d_r} = (J_2 + J_{2b})\ddot{\theta}_2 \quad (14)$$

$$T_{g2} = T_{fc} - J_{1b}\ddot{\theta}_{1b} \quad (15)$$

$$\ddot{\theta}_{1b} = \ddot{\theta}_2 i_2 \quad (16)$$

$$T_{g2} = T_{fc} - J_{ib}\ddot{\theta}_2 i_2 \quad (17)$$

where T_{g1} and T_{g2} are the primary and secondary shaft torque, T_{fc} is the friction clutch torque, T_{d_r} is the differential torque, J_{1b} and J_{2b} are the moment of inertia friction clutch and sprag clutch, J_2 is the moment of inertia of the secondary shaft, i_1 and i_2 are the gear ratios for the first and second gears, $\ddot{\theta}_{1b}$ is the angular acceleration of the friction clutch and $\ddot{\theta}_2$ is the angular acceleration of the secondary shaft, η_1 and η_2 are the first and the second gear efficiencies. Combining eq. (14) and eq.(17), it gives a form

$$Tg1i1\eta1 + Tfci2\eta2 - Jib\ddot{\theta}2i2^2\eta2 - Td_r = (J2 + J2b)\ddot{\theta}2 \quad (18)$$

Where $\ddot{\theta}_2 = \ddot{\theta}_m / i_1$ and $\ddot{\theta}_m = \ddot{\theta}_{d_r} i_{d_r} i_1$

$$Tg1i1\eta1 - Td_r + Tfci2\eta2 - J1b\ddot{\theta}2i2^2\eta2 = (J2 + J2b)\ddot{\theta}d_r id_r \quad (19)$$

Substituting equation will give the result as

$$Td_r = [Tm - Tfc - (Jm + j1)\ddot{\theta}d_r id_r i1]i1\eta1 + Tfci2\eta2 - J1b\ddot{\theta}1bi2\eta2 - (J2 + J2b)\ddot{\theta}d_r id_r \quad (20)$$

where J_2 is the moment inertia of secondary shaft, i_1 and i_2 are the transmission ratio of the first and secondary gear.

2.3 Chassis Model

For ride analysis, it is necessary to consider the wheel and suspension as a lumped mass (namely unsprung mass), whilst the vehicle body (sprung mass) is another lumped mass. The sprung mass governing equations (longitudinal displacement, vertical displacement and pitch angle) will be described initially, followed by the unsprung mass governing equations (vertical displacement of the unsprung mass and dynamic load transfer).

Sprung Mass Model:

For single mass representation, the vehicle body is assumed as a mass concentrated at its centre of gravity (G_{sm}). The point mass at the centre of gravity, with appropriate rotational moments of inertia, is dynamically equivalent to the vehicle body itself for all motions in which it is reasonable to assume the vehicle body to be rigid (Nizar and Mats 2017).

The aim of the model in this section is to analysis the longitudinal acceleration, vehicle speed, vertical displacement and pitch angle.

Longitudinal Force Balance for the Sprung Mass:

The longitudinal acceleration is found from the force balance sprung mass equation. The external forces resistances that affect the dynamic of the sprung

mass are also included. The force balance is satisfied by the equation,

$$F_{jx_{f,R}} + F_{jx_{f,L}} + F_{jx_{r,R}} + F_{jx_{r,L}} - m_{sm}\ddot{X}_{sm} - F_{aer} - F_{inc} = 0 \quad (21)$$

The longitudinal acceleration of the sprung mass is expressed as:

$$\ddot{X}_{sm} = \frac{\sum_{i=R,L} F_{jx_{f,i}} + \sum_{i=R,L} F_{jx_{r,i}} - F_{aer} - F_{inc}}{m_{sm}} \quad (22)$$

where F_{jx_f} and F_{jx_r} are the front and rear traction horizontal forces which from the tyres are transmitted to the vehicle through the suspension joints on the front and rear, m_{sm} is the mass of the sprung mass, $\ddot{X}_{sm}$ is the longitudinal acceleration of the sprung mass, F_{aer} and F_{inc} are the aerodynamic drag and the inclination resistance forces respectively. Subscript "R" and "L" denote the right and left side of longitudinal traction forces.

The aerodynamic drag resistance force is calculated as

$$F_{aer} = 0.5\rho_a A C_d \dot{\theta}_v^2 R_w^2 \quad (23)$$

where ρa is air density, C_d is the drag coefficient, A is the vehicle cross section area, $\dot{\theta}_v$ is the vehicle angular velocity and R_w is the wheel radius. And the inclination resistance force is calculated as,

$$F_{incl} = M_v g \sin\varphi \quad (24)$$

where M_v is the vehicle mass, g is the gravity acceleration and φ the road inclination. It is noted that the longitudinal acceleration of the sprung mass denoted as $\ddot{X}_{sm}$ that is the vehicle longitudinal acceleration. Hence, the jerk parameter of the vehicle is equal to the derivative of the longitudinal acceleration, equation (22).

3 SIMULATION RESULT

The sensitivity analysis is done by changing the input parameters predicted to affect the vehicle dynamic behavior during transient condition. The parameters of the HEV powertrain such as the power capacity of the power sources, the transmission gear ratio, torque distribution and the capacity of battery have significant influence on the vehicle performance and operating efficiency (Kyoungcheol, and Hyunsoo, 2017). These parameters will be taken into account as inputs for the sensitivity analysis with the exception of the capacity of battery. In the case of the parallel 4WD HEV, the effect of varying torque distribution is important when considering the interaction of two powertrains to produce a desired or undesired dynamic response.

In order to analyze the effect of torque distribution for the vehicle dynamics response, all combinations of the selected gear (front and rear transmission) should be presented however, some of the combinations can be represented by others as their responsiveness trends are similar. Therefore, only one combination of the selected gears are chosen to be presented and evaluated. The front transmission, first gear and rear transmission, second gear

The torque distribution ratio was designed starting from 100% ICE: 0% EM up to 0% ICE: 100% EM by decreasing the ICE by 20% and increasing the EM by 20% at every step. Because the overall value of wheel torque (the total torque front and rear axles) remains the same, the torque demand ratio for each certain torque distribution is determined by the selected gear and the power capacity of two powertrains.

The vehicle dynamic response parameters (as the output of the sensitivity analysis) observed during the tip-in test include the longitudinal acceleration, jerk, speed, pitch angle and vertical displacement of sprung mass.

Sensitivity Analysis:

In this case the vehicle was arranged to move with the initial speed 19 km/h in the selected gear 1/2, and then the tip-in test was performed with varying torque distribution for sensitivity-analysis.

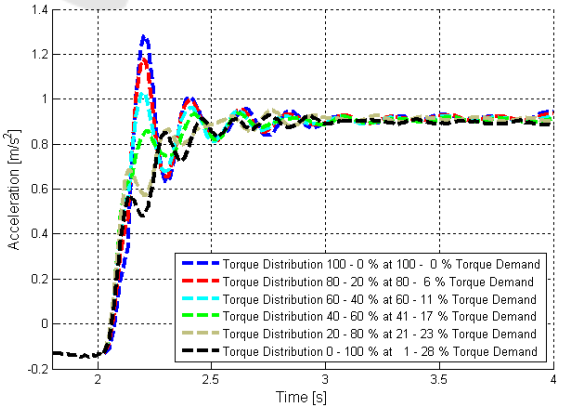

Figure 3: Sensitivity analysis of the longitudinal acceleration during a tip-in test with the initial vehicle speed 19 km/h and the selected gear 1/2.

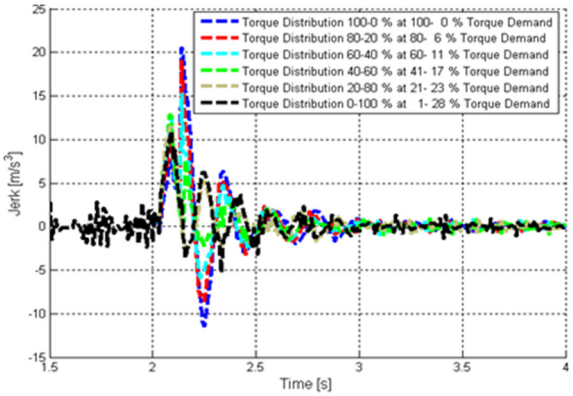

Figure 4: Sensitivity analysis of the jerk during a tip-in test with the initial vehicle speed 19 km/h and the selected gear 1/2.

Figure 3 shows varying responses of the vehicle longitudinal accelerations. It shows an increase of the acceleration oscillation for an increase of the engine driven axle torque and torque demand. The electric motor driven axle gives a small rise in oscillation and low amplitude oscillation during this test whilst the engine driven axle generates significant high amplitude oscillation. It is shown in Figure 3 that when the torque distribution of the EM is dominant, the maximum torque demand is needed only up to 28%. Figure 4 shows the jerk characteristics with different torque distributions. The results are similar to those for the acceleration. The increased jerk oscillation values are obtained when the engine torques are dominant compared to the electric motor torque demand and vice versa. The maximum jerk which can be reached when the torque distribution 80% ICE: 20% EM is 20 m/s^3 whereas for the torque distribution 20% ICE: 80% EM is approximately 12 m/s^3. Figure 5 shows the speed profiles for two manoeuvres where the torque distribution on the front and rear is 80:20% ICE:EM, and. The speed of different components at the wheel, such as the engine and electric motor, are referred to the vehicle speed (i.e. the engine speed is divided by selected gear ratio and differential ratio and multiplied by the wheel radius). As a consequence, the figure shows the concurrent evaluation of the torsion dynamics of both powertrain during the test.

Due to the initial torsion of the engine clutch damper and the inside of the component, the speed of the engine driven axle at the wheel tends to oscillate before the first set of clutch springs starts to transmit the torque. The simulation results show that each couple of speeds (engine with front wheel speed and motor with rear wheel speed) tends to converge at the end of the transient condition when the half-

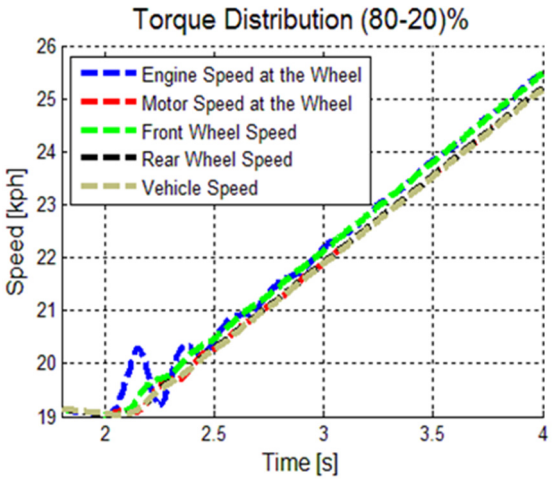

Figure 5: Speed comparison for each component speed referred to the vehicle speed during a tip-in test with the selected gear 1/2.

shaft reaches the steady-state torsion angle for that value of transmitted torque. In both figures, the tyre slip ratio dynamics are evident from the difference between the vehicle speed and the respective wheel speed. As a result of the transient condition, the wheel speed profile is higher on the axle transmitting the majority of the torque, the front axle in Figure 4.

4 CONCLUSIONS

After the development of a model and following the simulation, it is shown that the combination of the torque characteristics of the ICE and the EM propulsion and their transmission has the largest impact on driveline responses, which affect drivability. In addition, the vehicle dynamic response behavior has high oscillations and a more complex time history during hybrid mode due to the combination of rapidly variable torque demand and the first natural frequencies from two different propulsions in transient condition.

ACKNOWLEDGEMENTS

I wish to thank to all my colloquies in the Mechanical Department for involving during the study. Thank to Director of the State Polytechnic Ujung Pandang for providing facilities, and The Higher Education Ministry of Indonesia (Direktorat Riset dan Pengabdian Masyarakat, DRPM) for supporting the research funding.

REFERENCES

Giancarlo Genta and Lorenzo Morella, (2019). The Automotive Chassis Volume 2: System Design, p 429, Springer.

Liao, G. Y., Weber T. R. and Pfaff, D. P. (2004). Modelling and Analysis of Powertrain Hybridization on All-Wheel-drive Sport Utility Vehicles. *Proceeding Instn Mech. Engrs Vol. 218 Part D: Journal Automobile Engineering*.

Rizzoni, G., Guzzella, L., and Bernd, M. B. (2019). Unified Modelling of Hybrid Electric Vehicle Drivetrains. *IEEE/ASME Transactions on mechatronics*. Vol. 4, No. 3.

Velazquez Alcantar J. & Assadian F. (2019). Vehicle dynamics control of an electric-all-wheel- drive hybrid electric vehicle using tyre force optimisation and allocation, Vehicle System Dynamics, *International Journal of Vehicle Mechanics and Mobility*, DOI: 10.1080/00423114.2019.1585556.

Hohn B. R., Stahl K., Pflaum H., and Draxal T. (2011). Operating Experience with the Optimized CVT Hybrid Driveline. *Balkan Association of Power Transmissions*, Vol. 1, Issue 2, pp 32-38.

Cavallino C., and Turner A. (2009). Multi-Speed EV/FCV Transmission with Seamless Gearshift. *8th International CTI Symposium*, Innovative Automotive Transmissions.

Pacejka, H. B. (2006). Tyre and vehicle dynamics. Elsevier, 2nd Edition.

Holdstock T., Sorniotti A., Suryanto S., Leo S., Fabio V., and Carlo C. (2012). Linear and Nonlinear Methods to Analyse the Drivability of a Trough the Road Parallel Hybrid Electric Vehicle. *International Journal of Powertrain*.

Nizar Chaar and Mats Berg (2017). Simulation of vehicle–track interaction with flexible wheelsets, moving track models and field tests, Vehicle System Dynamics: *International Journal of Vehicle Mechanics and Mobility*, DOI: 10.1080/00423110600907667.

Kyoungcheol O., Junhong M., Donghoon C., and Hyunsoo K. (2017). Optimization of Control strategy for a single-shaft parallel hybrid electric vehicle. *Proceeding IMechE Vol. 221 Part D: J. Automobile Engineering*, DOI: 10.1243/09544070JAUTO93.